

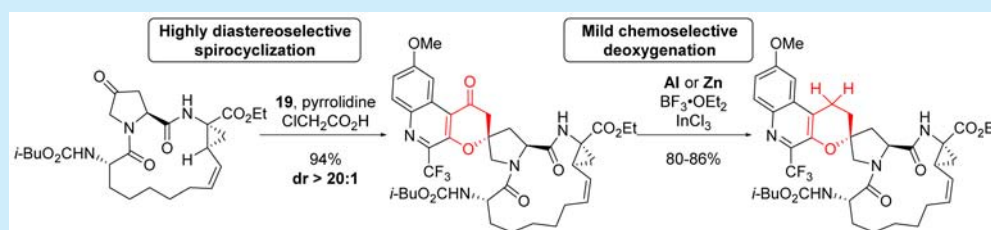
A Synthesis of a Spirocyclic Macrocyclic Protease Inhibitor for the Treatment of Hepatitis C

Cheol K. Chung,^{*,†} Ed Cleator,[‡] Aaron M. Dumas,[‡] Jacqueline D. Hicks,[†] Guy R. Humphrey,[†] Peter E. Maligres,[†] Andrew F. Nolting,[†] Nelo Rivera,[†] Rebecca T. Ruck,[†] and Michael Shevlin[†]

[†]Department of Process Chemistry, Merck Research Laboratories, Merck & Co., Inc., Rahway, New Jersey 07065, United States

[‡]Department of Process Chemistry, Merck Sharp and Dohme Ltd., Hertford Road, Hoddesdon EN11 9BU, United Kingdom

S Supporting Information



ABSTRACT: The development of a convergent and highly stereoselective synthesis of an HCV NS3/4a protease inhibitor possessing a unique spirocyclic and macrocyclic architecture is described. A late-stage spirocyclization strategy both enabled rapid structure–activity relationship studies in the drug discovery phase and simultaneously served as the basis for the large scale drug candidate preparation for clinical use. Also reported is the discovery of a novel InCl_3 -catalyzed carbonyl reduction with household aluminum foil or zinc powder as the terminal reductant.

Since the approval of the first series of direct acting antiviral agents by the FDA in 2011, the NS3/4A protease inhibitor has remained the crucial component in the Hepatitis C treatment regimen.¹ However, the rapid emergence of drug resistance, along with moderate sustained virological response with the initial treatment options, has led to intensified development efforts toward more potent antivirals with higher barriers to drug resistance.² One such compound is MK-8831 (**1**), which is under evaluation as a potential treatment with a broader genotypic response (Figure 1).³ Structurally, in

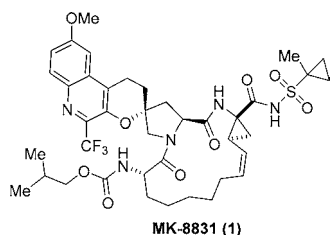


Figure 1. NS3/4a Protease inhibitor **1** for the treatment of Hepatitis C.

addition to the macrocyclic scaffold found in a number of second generation protease inhibitors such as grazoprevir,⁴ simeprevir,⁵ and danoprevir,⁶ MK-8831 contains a unique spirocyclic stereogenic center which is thought to provide favorable conformational rigidity, thereby enhancing the drug's binding affinity by lowering the entropic penalty arising from protein–ligand complex formation.⁷

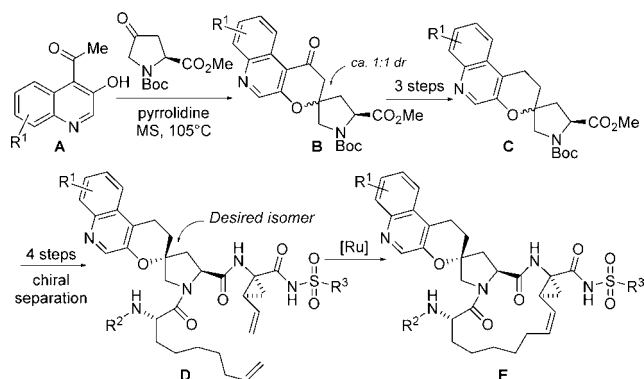
From a synthetic perspective, the spirocyclic design introduced significant complexity for the preparation of a large number of analogues for structure–activity relationship (SAR) evaluation. Therefore, it was highly desirable to design a synthetic strategy that would facilitate structural optimization and simultaneously provide an immediate path forward to large scale preparation. In this letter, we describe our efforts to enhance access to complex target compounds at the junction of discovery and process chemistry, and the evolution of this chemistry into an efficient kilogram-scale synthesis of compound **1**.

We began our investigation by examining the medicinal chemistry approach that utilized a late stage ring-closing metathesis to construct the 15-membered ring macrocycle with the preformed spirocycle **D** (Scheme 1). Since the quinoline moiety **A**, one of the key SAR components, was introduced at an early stage in a nonstereoselective manner and in a linear multistep sequence, the synthesis created a significant delay in the iterative lead optimization process. We envisioned a more convergent approach wherein two advanced intermediates were assembled stereoselectively at a late stage via an amine-mediated spirocyclization.⁸ In regard to the diastereoselectivity in the spirocyclization, we anticipated that the increased bulk of the proline fragment could favorably impact the diastereoselectivity-determining C–O bond formation.

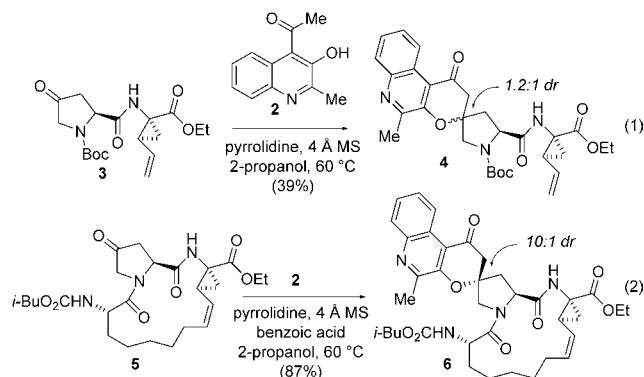
Received: February 1, 2016

Published: March 7, 2016

Scheme 1. Initial SAR Chemistry



Our initial efforts using the advanced intermediates such as amide **3** gave negligible improvement in diastereoselectivity indicating that the steric bias from the substituted amide group was insufficient to influence the selectivity (eq 1). To our



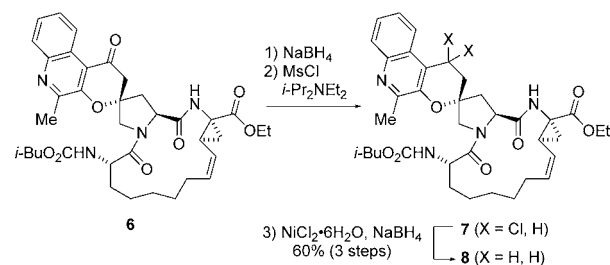
delight, however, the cyclization using the preformed macrocycle **5** provided the spirocyclic pyranone **6** in improved yield and diastereoselectivity toward the desired stereoisomer (60%, 5:1 dr). We found that the reaction could be further enhanced with an acid additive, improving the yield and diastereoselectivity to 87% and 10:1, respectively (eq 2).⁹

With proof-of-concept for late-stage spirocyclization in hand, our next challenge was to reduce the benzylic ketone to the corresponding methylene compound **8** chemoselectively in the presence of a number of sensitive functional groups such as an olefin, Boc group, ester, and cyclopropyl group. While all our initial deoxygenation attempts failed due to these chemoselectivity problems, we ultimately identified a mild three-step sequence involving ketone reduction, chlorination, and reductive dechlorination¹⁰ that allowed for smooth transformation of ketone to methylene in 60% overall yield, setting the stage for further SAR at the ester or amine functionality (Scheme 2).

The late stage spirocyclization–reduction strategy proved remarkably useful in expediting the SAR activity by allowing access to a variety of target compounds from the macrocyclic intermediate **5** in a few simple steps. More specifically, delaying the introduction of the quinoline fragment, which is the most complex diversifying element, was crucial in rendering the synthesis more convergent and amenable to parallel synthesis.

When the structural optimization efforts ultimately led to the identification of compound **1** as a drug candidate with a promising pan-genotypic profile, we started our development work by analyzing the existing synthesis to address any

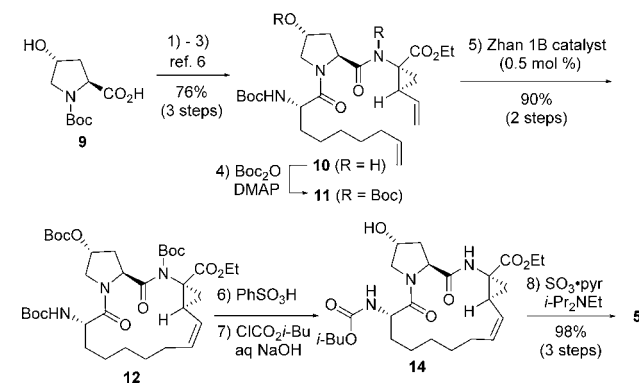
Scheme 2. Deoxygenation of Pyrone



potential challenges for large scale manufacturing. In our analysis, potentially problematic steps included the ring-closing metathesis (RCM) that required high catalyst loading, stannane-based Stille coupling used in the quinoline synthesis, and the multistep deoxygenation sequence.

The synthesis of the macrocycle-fused prolinone **5** started from known diene intermediate **11** (Scheme 3). During

Scheme 3. Preparation of Macrocycle 5



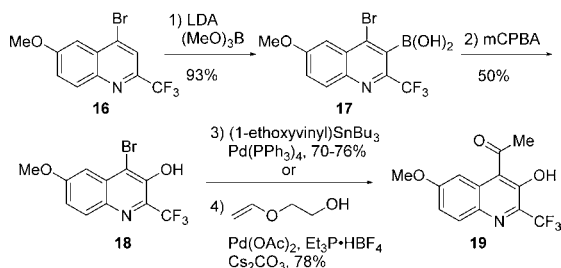
optimization of the RCM reaction, it became evident that the macrocyclization was not suitable for large scale preparation, requiring a high catalyst loading (>5 mol %) and high dilution (0.01–0.02 M) to afford the corresponding macrocycle in reasonable yield. In addition, the cyclization was accompanied by the formation of numerous oligomeric byproducts. This inefficiency was especially noticeable when the more reactive Grubbs–Hoveyda second generation catalyst was employed, implicating product participation in olefin metathesis. Further optimization efforts including higher concentration, elevated temperature, or slow addition of catalyst and/or substrate failed to provide a satisfactory improvement in reaction performance.

Postulating that the poor reactivity might be due to the presence of Lewis basic functional groups capable of sequestering the ruthenium catalyst, we adopted the method developed by Shu and co-workers and temporarily masked the proximal amide nitrogen with a Boc group.¹¹ Selective protection of the amide was not feasible due to facile O-Boc formation on the proline ring; therefore, we pursued the use of tri-Boc substrate **11** in the RCM reaction. To our gratification, diene **11** performed remarkably well at a catalyst loading as low as 0.5 mol %, providing the desired macrocycle **12** in 90% yield and >95% purity by HPLC analysis over 2 steps. The clean reaction profile in turn allowed us to carry the crude product forward to the subsequent transformation without purification. Global Boc deprotection, followed by carbamate formation provided the prolinol derivative **14**. Crude **14** was subjected to Parikh–Doering oxidation to afford prolinone **5**, which was

isolated as a crystalline solid in 98% overall yield from protected macrocycle **12**, constituting the single isolation point in an 8-step linear sequence.¹²

The quinoline **19** required for enamine-mediated spirocyclization was synthesized in three steps starting from bromoquinoline **16** (Scheme 4). Early route development

Scheme 4. Preparation of Quinoline **19**



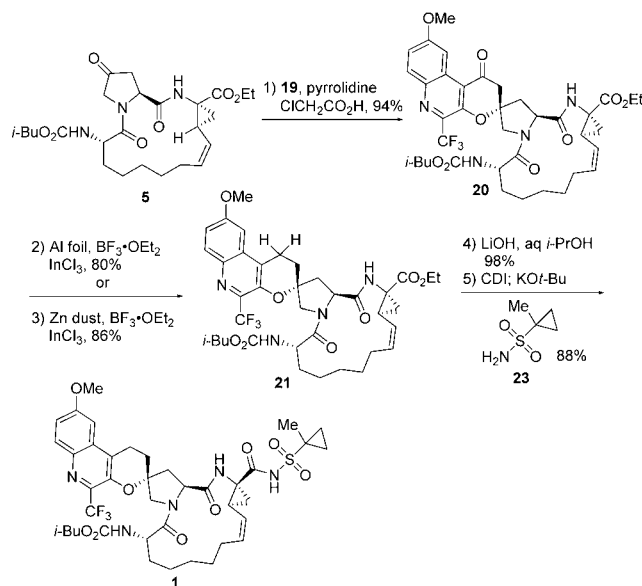
involving Stille coupling provided expedient access to the quinoline intermediate for the initial spirocyclization studies. For scale-up, we pursued an alternative acetylation method to avoid the toxicity issue associated with using a stoichiometric amount of tin reagent.

We envisioned that a properly regiocontrolled Heck coupling between the bromoquinoline **18** and a vinyl ether would serve as a practical alternative to Stille coupling.¹³ A variety of phosphine ligands and solvent combinations were evaluated in a high-throughput setting using Pd(OAc)₂ and ethylene glycol vinyl ether. Curiously, the Tedicyp ligand, which was reported to favor the linear isomer, proved most efficient in our screening, affording the branched product **19** exclusively in 87–89% LC assay yield.¹⁴ Et₃P was also effective, providing the desired product in 79–81% yield. Ultimately, Et₃P was selected for large scale application given its broader commercial availability (Scheme 4, step d). Product isolation was achieved by adding water to dissolve inorganics followed by acidification to crystallize the product directly from the reaction mixture in 78% yield.

Gratifyingly, the crucial spirocyclization between compounds **5** and **19** scaled very well with only minor modification. Optimization studies revealed that the product yield was higher with chloroacetic acid as an additive than with benzoic acid, and the cyclization was quite robust, tolerating up to 1 equiv of water obviating the need for molecular sieves.¹⁵ Aqueous workup, followed by recrystallization from toluene–heptane, provided the spirocycle product **20** in 94% yield as a single isomer (Scheme 5).

With the desired spirocycle product **20** in hand, our next focus was to improve the three-step deoxygenation sequence. Although it served the early stage small scale synthesis well, large scale preparation required safer, more robust methodology with operational simplicity. With these goals in mind, we conducted a series of high throughput experiments examining a variety of reduction methods.¹⁶ As observed previously, Wolff–Kishner-type conditions gave extensive decomposition, presumably due to the base sensitivity of the pyranone moiety. Silane-mediated reduction conditions were also revisited resulting in no reaction or complex mixtures. Finally, a screen of Clemmensen-type reduction conditions using a series of reducing metals, acids, and additives revealed that the combination of aluminum or zinc powder, BF₃·OEt₂, and a catalytic amount of InCl₃ as a viable chemoselective reducing

Scheme 5. Large Scale Synthesis of MK-8831 (**1**)



agent. Remarkably, shredded household aluminum foil in 2-propanol was identified as a highly effective terminal reductant. With a favorable Al/Al₂O₃ ratio, the use of foil significantly reduced the required amounts of aluminum and InCl₃ compared with aluminum powder. Under optimized conditions, the deoxygenation proceeded smoothly with 4.7 equiv of aluminum and 5.4 mol % InCl₃ at 40 °C. The product isolation was accomplished by removing the insoluble metal byproduct by filtration, aqueous workup, and crystallization from CPME–heptane to provide reduced compound **21** in 80% yield. Zinc-based reduction was found to be equally effective, especially for a larger scale, as the residual metal was more conveniently removed from fixed vessels. This Zn-based procedure afforded the desired product **21** in 86% yield on a 20 kg scale.¹⁷

The final coupling with sulfonamide **23** was accomplished via acyl imidazole using KOtBu as base in warm THF. The isolation of compound **1** required extensive investigation of its physical properties due to its tendency to form an amorphous solid, which made it difficult to completely remove impurities without reliance on column chromatography. While all our attempts at isolating compound **1** as a crystalline neutral solid or salt proved unsuccessful, a cocrystal screen identified a crystalline ethanol solvate of the potassium salt as well as an acetic acid solvate of neutral **1**. The latter proved effective at purging impurities and readily scalable, leading to its adoption for the final process. The final coupling step was successfully applied to multikilogram-scale synthesis providing MK-8831 in 88% yield and >99% purity, which was suitable for human safety studies.

In summary, we have described a practical large scale synthesis of MK-8831 (**1**) that utilizes a highly convergent and diastereoselective enamine-mediated spirocyclization and a novel InCl₃-catalyzed chemoselective deoxygenation reaction as key steps. Overall, the synthesis of compound **1** was achieved in 14 total steps and 43% yield from proline derivative **10** without column chromatography. The chemistry development strategy described here showcases our efforts to enable both rapid SAR in the drug discovery phase and bulk production of a

drug candidate facilitating its transition to the drug development stage.

■ ASSOCIATED CONTENT

Supporting Information

The Supporting Information is available free of charge on the ACS Publications website at DOI: [10.1021/acs.orglett.6b00331](https://doi.org/10.1021/acs.orglett.6b00331).

Experimental procedures, full characterization of all new compounds, copies of NMR spectra (PDF)

■ AUTHOR INFORMATION

Corresponding Author

*E-mail: cheol_chung@merck.com.

Notes

The authors declare no competing financial interest.

■ ACKNOWLEDGMENTS

We thank Robert Reamer and Ryan Cohen for their contribution in elucidating the stereochemistry of spirocyclic compounds.

■ REFERENCES

- (1) (a) Poordad, F.; McCone, J. J.; Bacon, B. R.; Bruno, S.; Manns, M. P.; Sulkowski, M. S.; Jacobson, I. M.; Reddy, K. R.; Goodman, Z. D.; Boparai, N.; Dinubile, M. J.; Sniukiene, V.; Brass, C. A.; Albrecht, J. K.; Bronowicki, J. *N. Engl. J. Med.* **2011**, *364*, 1195–1206. (b) Jacobson, I. M.; McHutchison, J. G.; Dusheiko, G.; DiBisceglie, A. M.; Reddy, K. R.; Bzowej, N. H.; Marcellin, P.; Muir, A. J.; Ferenci, P.; Flisiak, R.; George, J.; Rizzetto, M.; Shouval, D.; Sola, R.; Terg, R. A.; Yoshida, E. M.; Adda, N.; Bengtsson, L.; Sankoh, A. J.; Kieffer, T. L.; George, S.; Kauffman, R. S.; Zeuzem, S. *N. Engl. J. Med.* **2011**, *364*, 2405–2416.
- (2) Manns, M. P.; von Hahn, T. *Nat. Rev. Drug Discovery* **2013**, *12*, 595–610.
- (3) Neelamkavil, S. F.; Agrawal, S.; Bara, T.; Bennett, C.; Bhat, S.; Biswas, D.; Brockunier, L.; Buist, N.; Burnette, D.; Cartwright, M.; Chackalamannil, S.; Chase, R.; Chelliah, M.; Chen, A.; Clasby, M.; Colandrea, V. J.; Davies, I. W.; Eagen, K.; Guo, Z.; Han, Y.; Howe, J.; Jayne, C.; Josien, H.; Kargman, S.; Marcantonio, K.; Miao, S.; Miller, R.; Nolting, A.; Pinto, P.; Rajagopalan, M.; Ruck, R. T.; Shah, U.; Soriano, A.; Sperbeck, D.; Velazquez, F.; Wu, J.; Xia, Y.; Venkatraman, S. *ACS Med. Chem. Lett.* **2016**, *7*, 111–116.
- (4) Harper, S.; McCauley, J. A.; Rudd, M. T.; Ferrara, M.; DiFilippo, M.; Crescenzi, B.; Koch, U.; Petrocchi, A.; Holloway, M. K.; Butcher, J. W.; Romano, J. J.; Bush, K. J.; Gilbert, K. F.; McIntyre, C. J.; Nguyen, K. T.; Nizi, E.; Carroll, S. S.; Ludmerer, S. W.; Burlein, C.; DiMuzio, J. M.; Graham, D. J.; McHale, C. M.; Stahlhut, M. W.; Olsen, D. B.; Monteagudo, E.; Cianetti, S.; Giuliano, C.; Pucci, V.; Trainor, N.; Fandozzi, C. M.; Rowley, M.; Coleman, P. J.; Vacca, J. P.; Summa, V.; Liverton, N. J. *ACS Med. Chem. Lett.* **2012**, *3*, 332–336.
- (5) Rosenquist, Å.; Samuelsson, B.; Johansson, P.; Cummings, M. D.; Lenz, O.; Raboisson, P.; Simmen, K.; Vendeville, S.; Kock, H.; De Nilsson, M.; Horvath, A.; Kalmeijer, R.; De Rosa, G.; Beumont-mauviel, M. *J. Med. Chem.* **2014**, *57*, 1673–1693.
- (6) Jiang, Y.; Andrews, S. W.; Condroski, K. R.; Buckman, B.; Serebryany, V.; Wenglowksy, S.; Kennedy, A. L.; Madduru, M. R.; Wang, B.; Lyon, M.; Doherty, G. A.; Woodard, B. T.; Lemieux, C.; Do, M. G.; Zhang, H.; Ballard, J.; Vigers, G.; Brandhuber, B. J.; Stengel, P.; Josey, J. A.; Beigelman, L.; Blatt, L.; Seiwert, S. D. *J. Med. Chem.* **2014**, *57*, 1753–1769.
- (7) Zheng, Y.; Tice, C. M.; Singh, S. B. *Bioorg. Med. Chem. Lett.* **2014**, *24*, 3673–3682.
- (8) Kabbe, H. J. *Synthesis* **1978**, *1978*, 886–887.
- (9) For a similar Brønsted acid effect in proline catalysis, see: (a) Gryko, D.; Zimnicka, M.; Lipiński, R. *J. Org. Chem.* **2007**, *72*, 964–

970. (b) Magar, K. B. S.; Xia, L.; Lee, Y. R. *Chem. Commun.* **2015**, *51*, 8592–8595.

(10) Sarma, J. C.; Borbaruah, M.; Sharma, R. P. *Tetrahedron Lett.* **1985**, *26*, 4657–4660.

(11) Shu, C.; Zeng, X.; Hao, M.-H.; Wei, X.; Yee, N. K.; Busacca, C. A.; Han, Z.; Farina, V.; Senanayake, C. H. *Org. Lett.* **2008**, *10*, 1303–1306.

(12) Parikh, J. R.; Doering, W. v. E. *J. Am. Chem. Soc.* **1967**, *89*, 5505–5507. In our hands, other oxidation methods such as Dess-Martin periodinane and TEMPO-catalyzed oxidation provided low conversion or a poor impurity profile.

(13) (a) Hyder, Z.; Ruan, J.; Xiao, J. *Chem. - Eur. J.* **2008**, *14*, 5555–5566. (b) Arvela, R. K.; Pasquini, S.; Larhed, M. *J. Org. Chem.* **2007**, *72*, 6390–6396.

(14) Kondolff, I.; Doucet, H.; Santelli, M. *Eur. J. Org. Chem.* **2006**, *2006*, 765–774.

(15) Conversely, too much acid additive or continued exposure to air resulted in a lower yield (yield dropped by 30% and 20%, respectively).

(16) For reviews on various reduction methods, see: (a) Hutchins, R. O.; Hutchins, M. K. In *Comprehensive Organic Synthesis*; Trost, B. M., Ed.; Pergamon Press: Oxford, U.K., 1991; Vol. 8, pp 327–362. (b) Larson, G. L.; Fry, J. L. *Org. React.* **2008**, *71*, 1–737. (c) Vedejs, E. *Org. React.* **1975**, *22*, 401–422.

(17) Deuterium-labelling experiments support a Clemmensen-like mechanism with the alcohol solvent serving as the proton source. See Supporting Information for details.